

RESEARCH ARTICLE

Geometric calibration of a stationary digital breast tomosynthesis system based on distributed carbon nanotube X-ray source arrays

Changhui Jiang^{1,2☯‡}, Na Zhang^{1,2☯‡}, Juan Gao¹, Zhanli Hu^{1*}

1 Lauterbur Research Center for Biomedical Imaging, Shenzhen Institutes of Advanced Technology, Chinese Academy of Sciences, Shenzhen, China, **2** Shenzhen College of Advanced Technology, University of Chinese Academy of Sciences, Shenzhen, China

☯ These authors contributed equally to this work.

‡ These authors are co-first authors on this work.

* zl.hu@siat.ac.cn



OPEN ACCESS

Citation: Jiang C, Zhang N, Gao J, Hu Z (2017) Geometric calibration of a stationary digital breast tomosynthesis system based on distributed carbon nanotube X-ray source arrays. *PLoS ONE* 12(11): e0188367. <https://doi.org/10.1371/journal.pone.0188367>

Editor: Le Zhang, Sichuan University, CHINA

Received: October 11, 2017

Accepted: October 23, 2017

Published: November 29, 2017

Copyright: © 2017 Jiang et al. This is an open access article distributed under the terms of the [Creative Commons Attribution License](https://creativecommons.org/licenses/by/4.0/), which permits unrestricted use, distribution, and reproduction in any medium, provided the original author and source are credited.

Data Availability Statement: The datasets generated or analyzed during the current study are available at <https://figshare.com/s/96d8a1ef9c537f74411c>.

Funding: This work was supported in part by the National Natural Science Foundation of China (81401410, 81527804, 11575285), the Natural Science Foundation of Guangdong Province in China (2017A030313743), the Shenzhen Overseas High-Level Talent Peacock Team of China (KQTD2016053117113327), the Basic Research Program of Shenzhen in China

Abstract

Stationary digital breast tomosynthesis (sDBT) with distributed X-ray sources based on carbon nanotube (CNT) field emission cathodes has been recently proposed as an approach that can prevent motion blur produced by traditional DBT systems. In this paper, we simulate a geometric calibration method based on a proposed multi-source CNT X-ray sDBT system. This method is a projection matrix-based approach with seven geometric parameters, all of which can be obtained from only one projection datum of the phantom. To our knowledge, this study reports the first application of this approach in a CNT-based multi-beam X-ray sDBT system. The simulation results showed that the extracted geometric parameters from the calculated projection matrix are extremely close to the input values and that the proposed method is effective and reliable for a square sDBT system. In addition, a traditional cone-beam computed tomography (CT) system was also simulated, and the uncalibrated and calibrated geometric parameters were used in image reconstruction based on the filtered back-projection (FBP) method. The results indicated that the images reconstructed with calibrated geometric parameters have fewer artifacts and are closer to the reference image. All the simulation tests showed that this geometric calibration method is optimized for sDBT systems but can also be applied to other application-specific CT imaging systems.

Introduction

Traditional digital breast tomosynthesis (DBT) systems have been widely used, as such systems can overcome the overlapping phenomenon associated with mammography and can allow for differentiation between normal and pathological tissues on standard 2D projections in clinical settings[1–3]. However, the performance of traditional DBT is flawed; in particular, during a single scan, the X-ray tube moves along an arc and acquires few 2D projections within a

(JCYJ20160608153434110, JCYJ20150831154213680), the Applied Science and Technology Project of Guangdong Province in China (2015B020233014), the Key Laboratory for Magnetic Resonance and Multimodality Imaging of Guangdong Province (2014B030301013).

Competing interests: The authors have declared that no competing interests exist.

limited angle[4]. This movement causes instability in the system gantry, resulting in the appearance of severe artifacts in the reconstructed computed tomography (CT) images. In recent years, stationary DBT (sDBT) systems have been proposed to solve this problem. Qian *et al.* reported a sDBT system that uses a carbon nanotube (CNT)-based multi-beam field emission X-ray (MBFEX) source[5]. Quan *et al.* presented a multi-beam system that uses linear arrays of X-ray sources arranged in a square geometry[6]. Square sDBT systems include two arrays of CNT X-ray sources and two panel detectors in a rectangular arrangement. During one scanning cycle, the object phantom remains stationary, and neither the linear array sources nor the panel detectors are rotated. Using this approach and device can solve the motion artifact problem associated with traditional DBT scanners that is caused by rotation of the mechanical gantry during scanning. The use of square sDBT systems can significantly improve imaging quality. Other potential advantages of sDBT systems relative to other DBT systems include reduced total imaging time and simplified system design[7]. However, for such systems, errors during manufacturing and assembly are difficult to avoid due to the use of multiple CNT sources. These errors affect the final quality of the reconstructed images and can result in severe artifacts in CT images. Thus, to obtain the perfect geometric parameters for an imaging system, accurate geometric calibration is necessary[8]. Accurate geometric parameters are also crucial for high-quality image reconstruction by CT systems[9].

After decades of research and development, various geometric calibration methods have been used for different X-ray imaging systems[10]. These methods can be classified as analytic calibration methods[11–18] and iterative optimization calibration methods[19–23] based on the algorithm used during the process of geometric calibration. In iterative optimization calibration methods, CT system parameters are estimated by calculating coordinate values and iteratively revising parameters from original estimates using various penalty terms. In analytic calibration methods, reconstruction parameters are obtained by directly calculating the elliptical geometries formed by combining all of the projection images obtained at different scanning angles. Analytic calibration methods are more commonly used in the field of CT reconstruction, as such methods have many advantages, including that they are easier to implement and require fewer calculations.

Geometric calibration methods can also be divided into phantom-based methods[12,18,24] and phantom-less methods[25–27] according to whether a customized or universal phantom is used in the process of geometric calibration. In phantom-based methods, to estimate geometric parameters, a calibration phantom consisting of certain numbers of markers must be used to acquire projections. A phantom-based calibration method can obtain geometric parameters based on the relationships between projected locations and the predefined positions of markers. The accuracy of such methods depends on the manufacturing precision of the calibration phantom. In phantom-less methods, no calibration phantom is utilized during the calibration process. Instead, geometric parameters are directly calculated from projection images, although these approaches involve expensive computational loads.

Each of the aforementioned methods has advantages and disadvantages. In this article, we report a simulation study of geometric calibration with a phantom-based method for a proposed multi-source CNT X-ray sDBT system. The method is a projection matrix-based approach in which only one projection datum of the phantom at an arbitrary incidence angle is required to obtain all geometric parameter information for the sDBT system with CNT X-ray sources and flat-panel detectors.

This paper is structured as follows. The methods and materials section provides a detailed description of a generic geometric calibration method based on projection matrices. In the results section, this method is applied to extract system geometric parameters of a sDBT system, and the geometric parameters were compared. To more intuitively test the accuracy of

the geometric algorithms, a traditional cone-beam CT (CBCT) system with installation error was also simulated. During the calibration process, a self-fabricated phantom with 8 ball markers was utilized to extract the geometric parameters of the CBCT system, and a modified Shepp-Logan phantom was used to obtain the projection data. Finally, the projection data was reconstructed based on a universal filtered back projection (FBP) algorithm with and without the calibrated geometrical parameters to evaluate the efficacy of the geometric calibration algorithm. In the conclusion section, the major findings of the study are summarized.

Methods and materials

In the simulation, the geometry of the examined sDBT system is composed of two linear arrays of CNT X-ray sources and two panel detectors. These four components form a square, as illustrated in Fig 1.

First, we specify seven important parameters of the sDBT system for image reconstruction (Fig 2): (u_0, v_0) , the coordinates of the orthogonal projection of an X-ray focal spot on the detector plane; SOD, the distance from a source to the center of the square; SDD, the source-to-detector distance; η , the rotation angle of the detector plane along its normal vector; φ , the rotation angle of the detector plane along the $u = u_0$ axis; θ , the rotation angle of the detector plane along the $v = v_0$ axis; (X_s, Y_s, Z_s) , the coordinates of the sources; and (u, v) , the coordinates of the sources' projections on the detector.

These seven parameters are determined using the formulae described below. For additional details, please see reference [28]. In this square sDBT system (see Fig 1), the calibration process is identical for all CNT X-ray sources; therefore, we can consider one CNT source as an example to illustrate the geometric calibration principle.

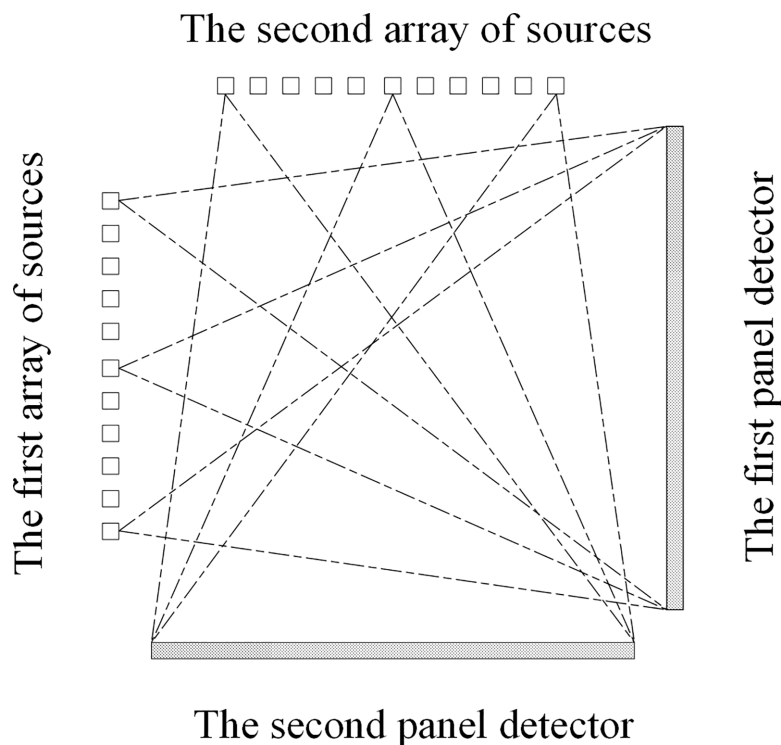


Fig 1. Schematic representation of the imaging geometry, with two linear arrays of CNT sources arranged opposite the detectors to form the rectangular sDBT system.

<https://doi.org/10.1371/journal.pone.0188367.g001>

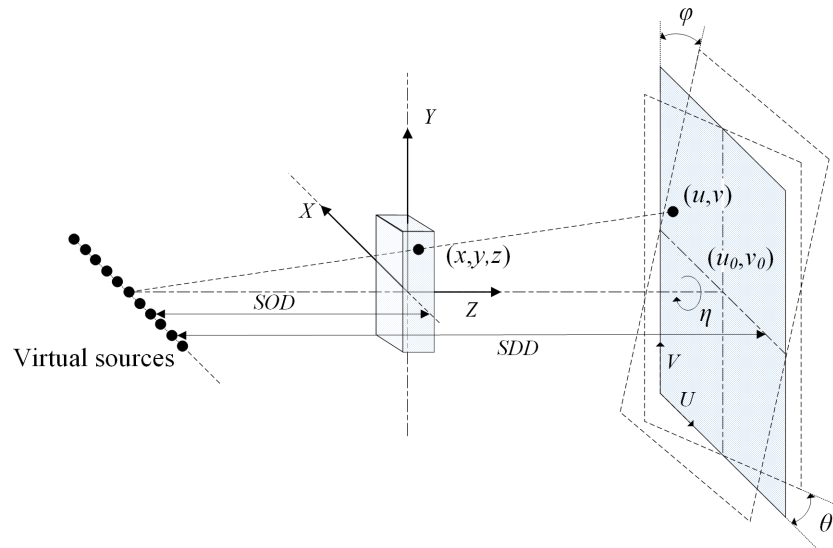


Fig 2. Schematic of the projection and coordinate system.

<https://doi.org/10.1371/journal.pone.0188367.g002>

A projection matrix is a 3×4 matrix that relates the mapping of a point (x, y, z) in object coordinates to its projection (u, v) on a two-dimensional detector defined using homogeneous coordinates:

$$[Ax, Ay, Az, A]^T = [au, av, a]^T \quad (1)$$

where α is an arbitrary scaling factor. The projection matrix A can be factorized as:

$$A = K[S|t] \quad (2)$$

where K is a 3×3 upper triangular matrix, S is a 3×3 rotation matrix, and t is a 3×1 translation vector.

$$K = \begin{bmatrix} \frac{SDD}{\lambda} & 0 & u_0 \\ 0 & \frac{SDD}{\lambda} & v_0 \\ 0 & 0 & 1 \end{bmatrix} \quad (3)$$

where u_0 and v_0 are the coordinates of the intersection point associated with the central ray and the detector, and λ is the detector pixel size. The parameter S can be further represented using three Euler angles or a unitary quaternion:

$$S = \begin{bmatrix} \cos\eta\cos\phi & \sin\theta\cos\eta\sin\phi - \cos\theta\sin\eta & \sin\phi\cos\theta\cos\eta + \sin\eta\sin\theta \\ \sin\eta\cos\phi & \sin\theta\sin\eta\sin\phi + \cos\theta\sin\eta & \sin\eta\cos\theta\cos\phi - \cos\eta\sin\theta \\ -\sin\phi & \cos\phi\sin\theta & \cos\phi\cos\theta \end{bmatrix} \quad (4)$$

The three Euler angles η , φ and θ represent the orientation of the detector plane in the object frame. In formula (2), parameter t is:

$$t = \begin{bmatrix} t_1 \\ t_2 \\ t_3 \end{bmatrix} \tag{5}$$

Thus, u_0 and v_0 can be expressed explicitly. From formula (3):

$$u_0 = K_{13}, v_0 = K_{23} \tag{6}$$

The parameter source-to-object distance (SOD) is:

$$SOD = K_{11}\lambda \tag{7}$$

The rotation angles of the detector are:

$$\begin{aligned} \theta &= \text{Arc tan}2(S_{32}, S_{33}) \\ \varphi &= \sin^{-1}(-S_{31}) \\ \eta &= \text{Arc tan}2(S_{12}, S_{11}) \end{aligned} \tag{8}$$

The source position is:

$$o = [o_x, o_y, o_z]^T = -S^T t \tag{9}$$

where t is:

$$\begin{aligned} t_1 &= A_{34} \\ t_2 &= (A_{24} - K_{23}A_{34})/K_{22} \\ t_3 &= (A_{14} - t_{13}A_{34} - K_2A_{12})/K_{11} \end{aligned} \tag{10}$$

Thus, the SOD is:

$$SOD = \sqrt{(o_y)^2 + (o_x)^2 + (o_z)^2} \tag{11}$$

To extract geometric parameters of the sDBT system, we designed a calibration phantom that contains 8 ball markers, each of which has a diameter of 10 units. In a realistic system, there are many possible arrangements of these markers in the phantom. To simplify the implementation of our calibration method, we designed the calibration phantom as shown in Fig 3 (A). The ball markers are arranged in two parallel planes with four balls in each plane, and the balls' coordinates and geometric parameters are known. To accurately calculate the seven geometric parameters mentioned above, it is extremely important to determine the exact center coordinates of these marker balls on the projection images. We use MATLAB programs to obtain the centers of the ball markers in the projection images via an approach based on a least squares and genetic algorithm. We then calculate the projection matrix of the square sDBT system for each CNT X-ray source-panel detector pair. Finally, the aforementioned calibration method based on a computer simulation is presented with a calibration phantom using Visual C++.

Specifically, the proposed geometric calibration method is implemented via the following steps. First, the phantom mentioned above is imported into the simulation model to imitate the acquisition of projection data. In the square sCBT system, which has 22 CNT X-ray sources distributed across two linear arrays, each CNT X-ray source is individually controlled, and

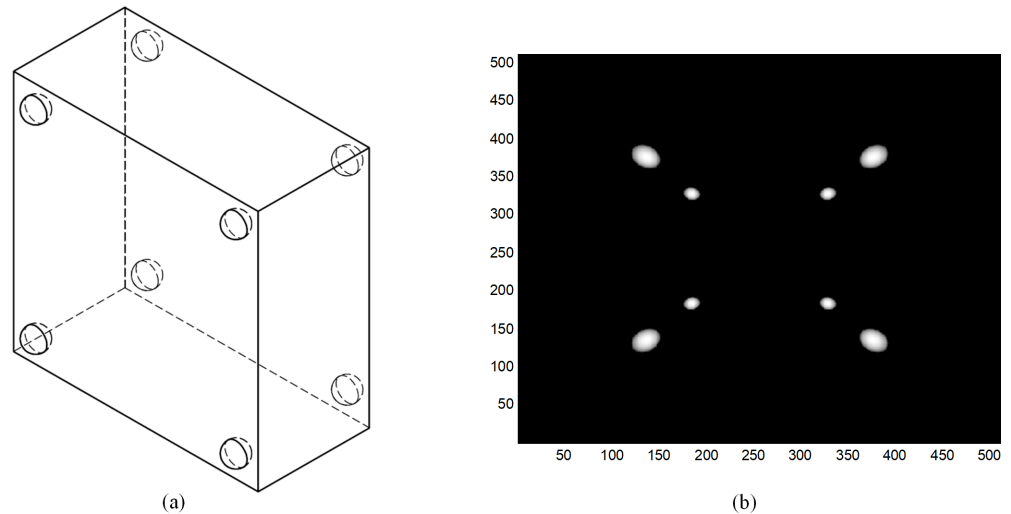


Fig 3. (a) Schematic of the calibration phantom. (b) Projection of the calibration phantom for individual emission by one of the CNT X-ray sources located in the middle.

<https://doi.org/10.1371/journal.pone.0188367.g003>

sources are switched on one by one. That is, at each time, only one source emits X-rays, and the detector acquires one projection image, as illustrated in Fig 3(B). In these projection images, the projections of the ball markers are elliptical. The center coordinates of these ellipses in the detector plane are then extracted. Finally, the projection matrix is calculated based on the mapping relationship between the known 3D coordinates of point markers and the 2D projection coordinates of these markers in the image plane. The seven aforementioned geometric parameters are then derived.

Results

Extracted geometrical parameters of the sDBT system and results analysis

For this simulation, we define all lengths in units of detector pixels. To reduce calculation requirements, each source array only contains 11 CNT X-ray sources that are equidistantly distributed across the linear array. The two arrays form two contiguous sides of a square in the transaxial plane. The length of the source array is 100, and two 512 (width) × 512 (height) flat-panel detectors form the other two sides of the square. The source-to-detector distance (SDD) is 200 units, and the SOD is 100 units. A coordinate system is defined as illustrated in Fig 2. During a scan, the object phantom remains stationary, and neither the two linear array sources nor the two panel detectors rotate.

To test the accuracy of the aforementioned geometrical calibration method, the phantom is simulated in the square sDBT system, as illustrated in Fig 4. We utilize the projection's 2D coordinates on the image detector and the previously known 3D coordinates of the ball markers to compute the geometric parameters. To demonstrate the results of the geometric calibration, the geometric parameters that are input into the simulation are compared with the extracted parameters. Because the calibration mechanisms of the two arrays of sources are completely identical, we can focus on the geometric calibration of the first array of sources and the corresponding detector. We take the 6th X-ray source (Fig 4) as an example to demonstrate the calibration process. The input parameters and extracted parameters for each CNT source are shown in Fig 5 and Table 1.

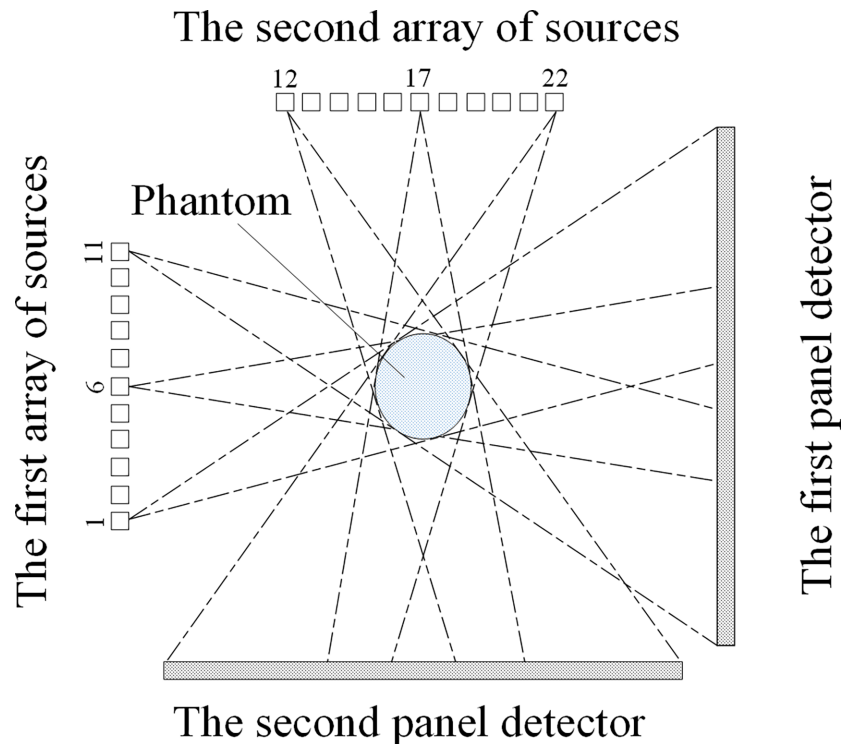


Fig 4. Schematic representation of the simulation projection process; the 22 CNT X-ray sources are numbered (1–22) and are sequentially triggered for emission.

<https://doi.org/10.1371/journal.pone.0188367.g004>

Fig 5 and Table 1 indicate that the extracted geometric parameters are extremely close to the input values, and most of the errors for the obtained values are less than 1 detector pixel unit, except the errors of the SDD. Moreover, the maximum error for the SDD is 1.2 pixel units, which is much smaller than the errors associated with actual mechanical installation. In this computer simulation experiment, the results obtained using the calibration method are extremely close to the corresponding actual values.

By repeating the above steps, we calculate the geometric parameters of the remaining CNT X-ray sources. The projections of the calibration phantom for these 22 CNT X-ray sources are shown in Fig 6. Finally, we can obtain all the geometric parameters of the square sDBT system.

Simulation tests of traditional cone-beam CT

The input geometric parameters and the extracted parameters are compared above. The experiments demonstrate that the extracted geometric parameters are quite close to the input values. To more intuitively test the accuracy of the geometric calibration algorithm, traditional CBCT with a flat-detector was simulated. The source and detector rotated synchronously while a stationary object was scanned. The SOD was set as 570 mm and the SDD as 1040 mm. The size of the flat-detector was 512×512. To simulate the installation error of the detector, the center of the detector was installed offset by 0, 1, 2, or 5 pixels.

The calibration process of the CBCT was as follows. First, a self-fabricated calibration phantom with 8 ball markers were utilized to extract the geometric parameters of the CBCT system, and four sets of geometric parameters were obtained. Then, a modified Shepp-Logan phantom is used to obtain the projection data during each scan, and four sets of projection data were obtained according to these four sets of geometric parameters. Finally, the projection data

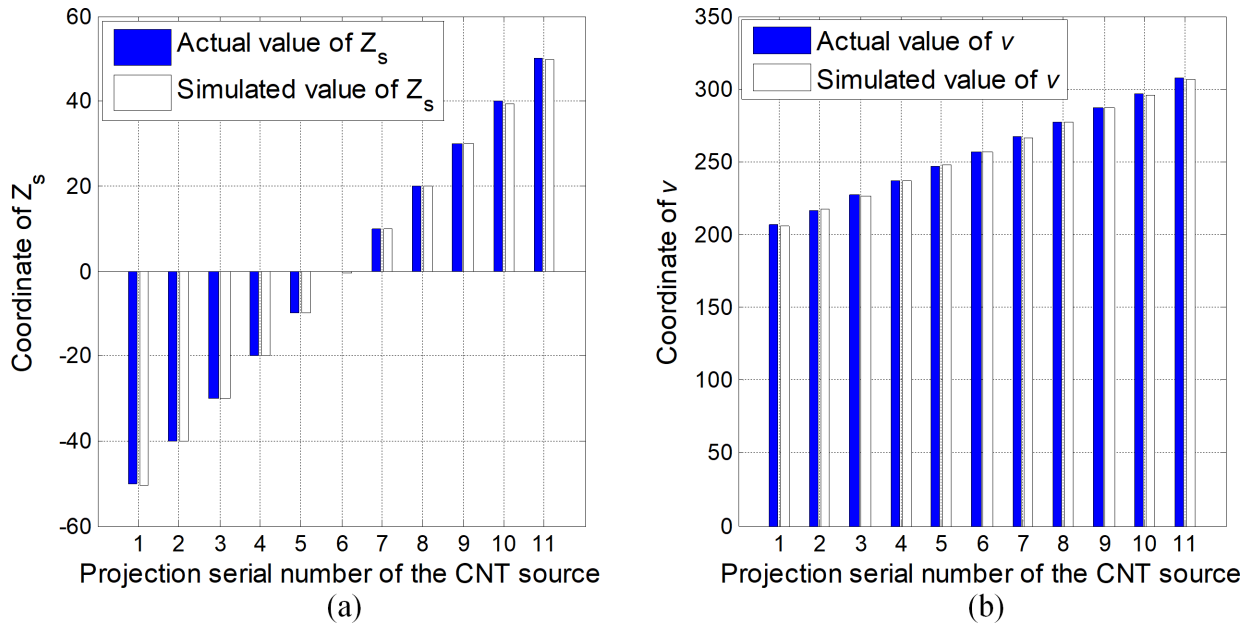


Fig 5. Comparisons of input values and extracted values of the coordinates of the CNT sources (Z_s) (a) and the coordinates of the sources' projections (v) (b).

<https://doi.org/10.1371/journal.pone.0188367.g005>

were reconstructed based on a universal filtered back projection (FBP) algorithm with and without the calibrated geometrical parameters to evaluate the efficacy of the geometric calibration algorithm.

As shown in Table 2 and Table 3, all the input geometric parameters and extracted parameters of the CBCT system are highly similar, except SDD, SOD and Y_s . In the simulated CBCT system, these three parameters described the distances between the X-ray source, the object and the detector. Although these three parameters seemed to have larger errors than other parameters, these errors empirically have limited influence on reconstructed images.

After the geometric parameters of the CBCT system were obtained, a modified 3D Shepp-Logan phantom was scanned, and 360 equally-spaced projections were obtained in one scanning circle. These projections were then used for image reconstruction based on the FBP method with the calibrated and uncalibrated geometric parameters.

Table 1. Comparisons of the input geometric parameters and the extracted simulation parameters.

		φ (deg)	θ (deg)	η (deg)	X_s	Y_s	SDD	SOD	u
Input parameters		0	0	90	0	-100	200	100	257
Extracted parameters	1	0.0472	0	90.0002	-0.463561	-99.2268	198.763	99.2268	256.258
	2	0.0397	0	90.0002	-0.466712	-99.8267	200.11	99.8563	256.25
	3	0.0562	0.1825	90.0002	-0.463561	-99.2268	198.763	99.2268	256.258
	4	0.0216	0	90.0002	-0.463561	-99.2268	198.763	99.2268	256.258
	5	0.0563	0	90.0002	-0.463561	-99.2268	198.763	99.2268	256.258
	6	0	0	90.0002	-0.463561	-99.2268	198.763	99.2268	256.258
	7	-0.011	0	90.0002	-0.463561	-99.2268	198.763	99.2268	256.258
	8	0	0	90.0002	-0.463561	-99.2268	198.763	99.2268	256.258
	9	-0.1738	-0.0002	90.0002	-0.463561	-99.2268	198.763	99.2268	256.258
	10	0.1287	0	90.0002	-0.463561	-99.2268	198.763	99.2268	256.258
	11	-0.0098	0.1591	90.0002	-0.463561	-99.2268	198.763	99.2268	256.258

<https://doi.org/10.1371/journal.pone.0188367.t001>

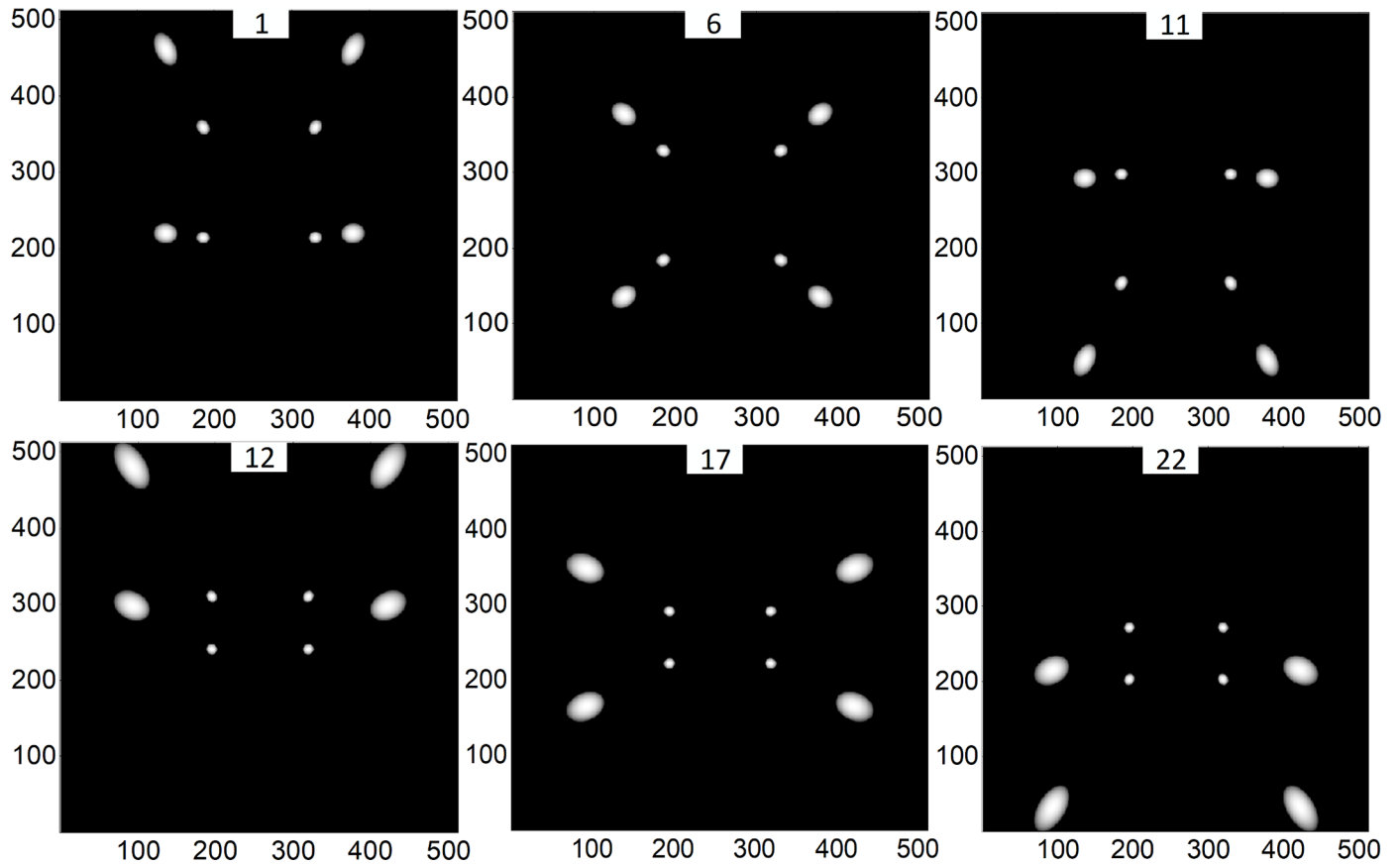


Fig 6. Projections of the calibration phantom for all CNT X-ray sources, taking the projections of the 1st, 6th, 11th, 12th, 17th and 22nd source (see Fig 4) as examples.

<https://doi.org/10.1371/journal.pone.0188367.g006>

Table 2. Comparisons of the set geometric parameters and the extracted simulation parameters.

	φ (deg)	θ (deg)	η (deg)	X_s (mm)	Y_s (mm)	Z_s (mm)	SDD (mm)	SOD (mm)
set parameters	0	0	90	0	-570	0	1040	570
0-pixel offset	0	0	90.0002	-0.00005	-565.385	-0.00005	1030.77	565.385
1-pixel offset	0	0	90.0002	0.00032	-565.385	-0.00005	1030.77	565.385
2-pixel offset	0	0	90.0002	-0.00028	-565.385	-0.00005	1030.77	565.385
5-pixel offset	0	0	90.0002	-0.00013	-565.385	-0.00005	1030.77	565.385

<https://doi.org/10.1371/journal.pone.0188367.t002>

Table 3. Comparisons of the set geometric parameters and the extracted simulation parameters of the coordinates of the sources' projections on the detector. (U_{set} , V_{set}) and (U_{ext} , V_{ext}) represent the set and extracted coordinates, respectively, of the sources' projections on the detector.

	U_{set}	U_{ext}	V_{set}	V_{ext}
0-pixel offset	257	257	257	257
1-pixel offset	258	258	257	257
2-pixel offset	259	259	257	257
5-pixel offset	262	262	257	257

<https://doi.org/10.1371/journal.pone.0188367.t003>

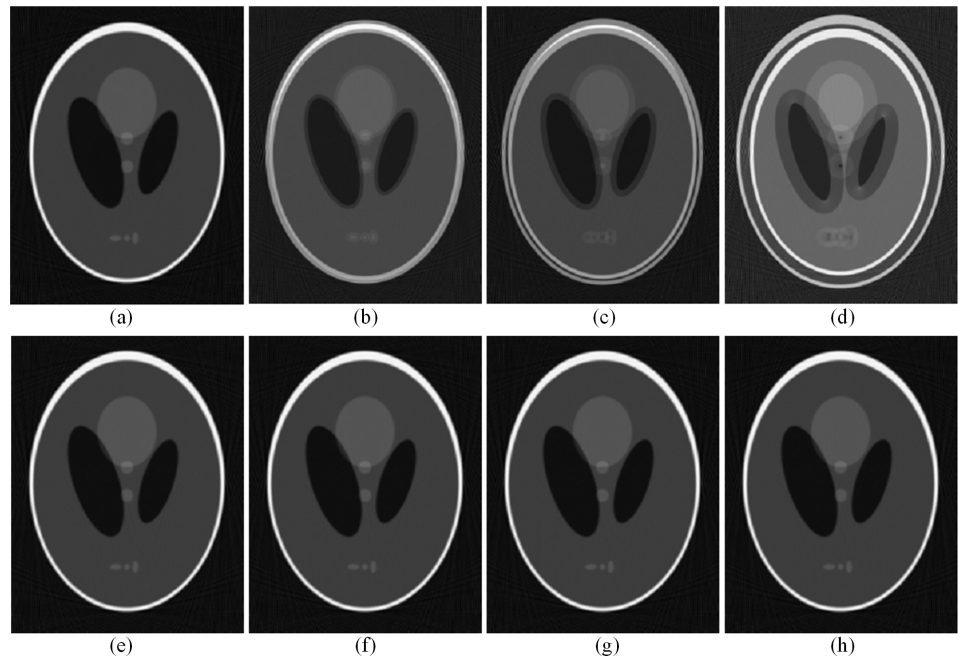


Fig 7. Reconstructed images using geometrical parameters with and without calibration. (a) A reconstructed image with input geometrical parameters without offset. [(b)-(d)] Reconstructed images with different offsets but without calibration. (b) offset = 1 pixel; (c) offset = 2 pixels; (d) offset = 5 pixels. (e) A reconstructed image with extracted geometrical parameters without offset. (f) The reconstructed image in (b) after calibration. (g) The reconstructed image in (c) after calibration. (h) The reconstructed image in (d) after calibration.

<https://doi.org/10.1371/journal.pone.0188367.g007>

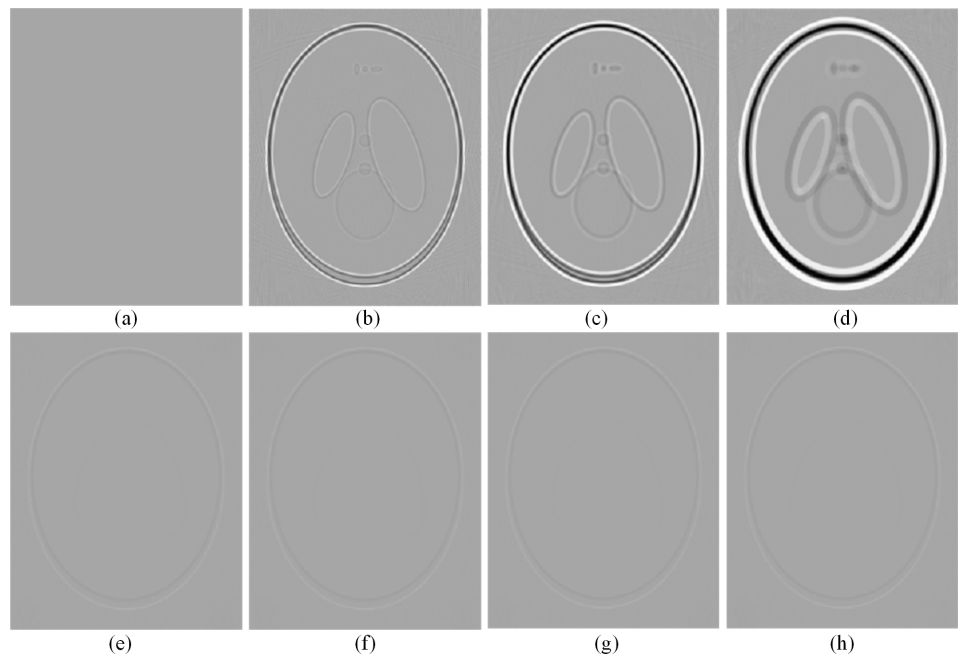


Fig 8. The residual images of the reconstructed results shown in Fig 7. The images are displayed in the window [-0.13 0.07].

<https://doi.org/10.1371/journal.pone.0188367.g008>

Four different CBCT systems with different mechanical installation errors were simulated. The FBP-reconstruction results of the modified Shepp-Logan phantom are shown in Fig 7. Images (a)~(d) of Fig 7 were reconstructed with the input geometrical parameters without calibration, and obvious artifacts were observed when the installation error was introduced into the imaging system. The reconstructed image for the 1-pixel offset is very blurred, the reconstructed image for the 2-pixel offset contains severe artifacts, and it is nearly impossible to distinguish any structural information of the reconstructed image for the 5-pixel offset. Images (e)~(h) were reconstructed with calibrated geometrical parameters, and the artifacts in these images caused by installation errors were effectively suppressed.

The image shown in Fig 7 (A) is a reconstructed image with input geometrical parameters and without offset, which was considered as the reference image. To quantitatively evaluate the reliability of the proposed algorithm, the profile images of the reconstructed images and the residual images with the reference image are shown in Fig 8 and Fig 9, respectively. The

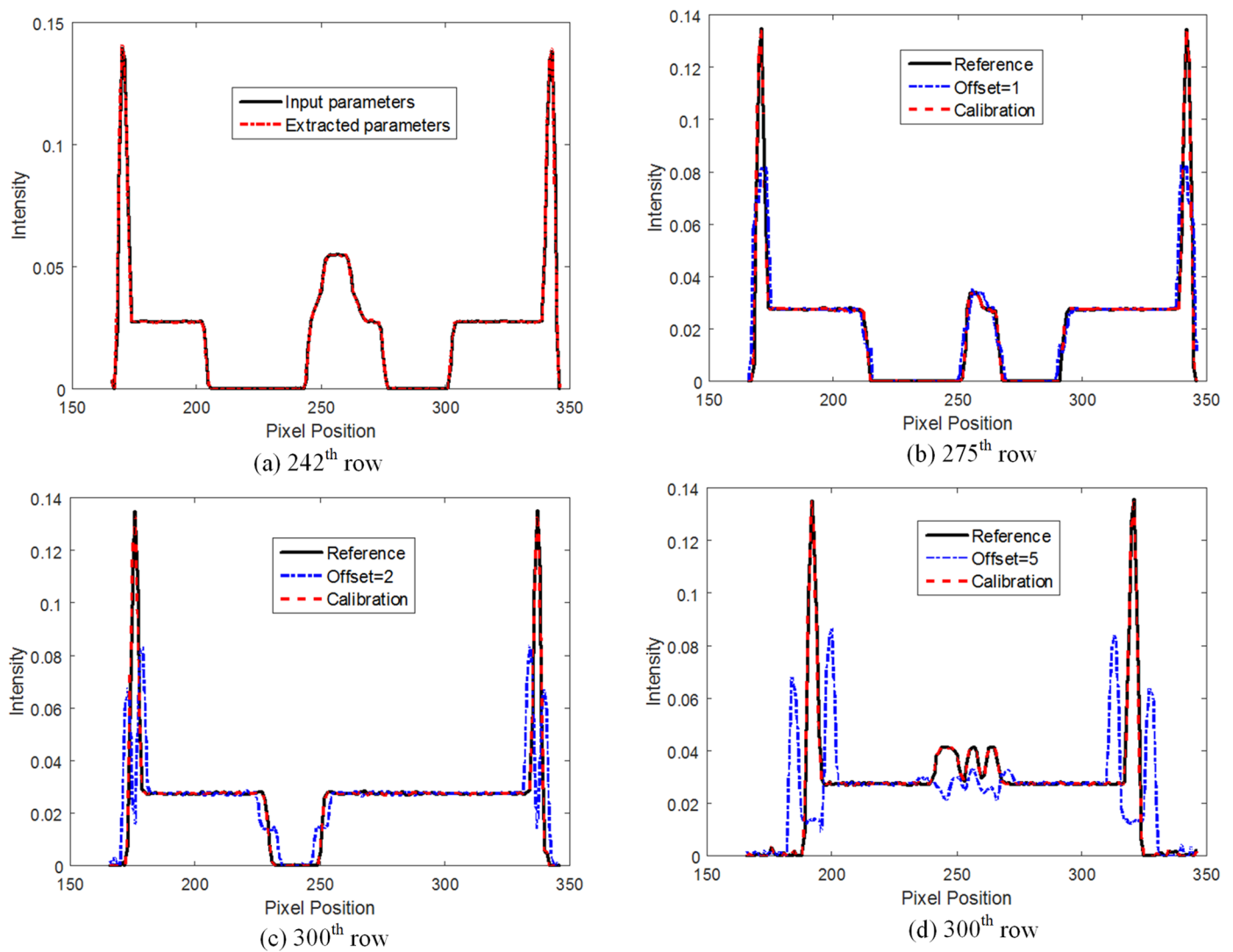


Fig 9. Profiles of different results shown in Fig 7. (a) Profile of the reconstructed images with input or extracted geometrical parameters without offset in the 242th row. (b) Profile of the reconstructed images with or without geometrical calibration with 1-pixel offset in the 275th row. (c) Profile of the reconstructed images with or without geometrical calibration with 2-pixel offset in the 300th row. (d) Profile of the reconstructed images with or without geometrical calibration with 5-pixel offset in the 335th row.

<https://doi.org/10.1371/journal.pone.0188367.g009>

results show that the proposed method can help achieve a superior image quality after reconstruction without calibration in terms of preserving the structure and suppressing undesired artifacts, which indicates its useful potential for CT imaging.

Conclusions

We developed a geometric calibration method based on a projection matrix approach for a square sDBT system and verified its performance. The errors of the input geometric parameters and the extracted parameters are compared based on the results of the geometric parameters extracted from the sDBT system. The simulations demonstrated that the extracted geometric parameters are quite close to the input values. Furthermore, to more intuitively test the accuracy of the geometric algorithms, traditional scanning in a circular manner using the CBCT system with a flat-detector was simulated. The reconstructed images with and without calibrated geometrical parameters were compared. The results indicated that the proposed algorithm can be used to extract the geometric parameters with sufficient accuracy for image reconstruction and can significantly reduce the artifacts caused by installation errors. In conclusion, the proposed calibration method not only can be used to extract the seven geometric parameters of the square sDBT system but can also be used in other traditional X-ray imaging systems, and these parameters were consistent with the corresponding actual input values with high numerical precision.

Supporting information

S1 File. The code of this manuscript. The datasets generated or analyzed during the current study are available at <https://figshare.com/s/96d8a1ef9c537f74411c>. (ZIP)

Acknowledgments

The authors would like to thank the editor and anonymous reviewers for their constructive comments and suggestions. This work was supported in part by the National Natural Science Foundation of China (81401410, 81527804, 11575285), the Natural Science Foundation of Guangdong Province in China (2017A030313743), the Shenzhen Overseas High-Level Talent Peacock Team of China (KQTD2016053117113327), the Basic Research Program of Shenzhen in China (JCYJ20160608153434110, JCYJ20150831154213680), the Applied Science and Technology Project of Guangdong Province in China (2015B020233014), the Key Laboratory for Magnetic Resonance and Multimodality Imaging of Guangdong Province (2014B030301013).

Author Contributions

Data curation: Changhui Jiang.

Methodology: Na Zhang, Zhanli Hu.

Software: Juan Gao.

Writing – review & editing: Na Zhang, Zhanli Hu.

References

1. Rafferty EA (2007) Digital mammography: novel applications. *Radiologic Clinics of North America* 45: 831–843. <https://doi.org/10.1016/j.rcl.2007.06.005> PMID: 17888772

2. Niklason LT, Christian BT, Niklason LE, Kopans DB, Castleberry DE, et al. (1997) Digital tomosynthesis in breast imaging. *Radiology* 205: 399. <https://doi.org/10.1148/radiology.205.2.9356620> PMID: 9356620
3. Bassett LW (2005) *Diagnosis of diseases of the breast*: Saunders. 2317–2320 p.
4. Gennaro G, Toledano A, Di Maggio C, Baldan E, Bezzon E, et al. (2010) Digital breast tomosynthesis versus digital mammography: a clinical performance study. *European radiology* 20: 1545–1553. <https://doi.org/10.1007/s00330-009-1699-5> PMID: 20033175
5. Qian X, Rajaram R, Calderon-Colon X, Yang G, Phan T, et al. (2009) Design and characterization of a spatially distributed multibeam field emission x-ray source for stationary digital breast tomosynthesis. *Medical Physics* 36: 4389–4399. <https://doi.org/10.1118/1.3213520> PMID: 19928069
6. Quan E, Lalush DS. EVALUATION OF HEXAGONAL AND SQUARE GEOMETRIES FOR MOTION-FREE ARRAYED-SOURCE X-RAY MICRO-CT; 2007. pp. 221–224.
7. Jenkins C, Rodríguez-Roisin R. Stationary digital breast tomosynthesis system with a multi-beam field emission x-ray source array; 2008. pp. A9131.
8. Hu ZL, Gui JB, Zou J, Rong JY, Zhang QY, et al. (2011) Geometric Calibration of a Micro-CT System and Performance for Insect Imaging. *Ieee Transactions on Information Technology in Biomedicine* 15: 655–660. <https://doi.org/10.1109/TITB.2011.2159012> PMID: 21659036
9. Barrett JF, Keat N (2004) Artifacts in CT: Recognition and avoidance. *Radiographics* 24: 1679–1691. <https://doi.org/10.1148/rg.246045065> PMID: 15537976
10. Yang Y, Li L, Chen ZQ (2016) A review of geometric calibration for different 3-D X-ray imaging systems. *Nuclear Science and Techniques* 27.
11. Bronnikov AV (1999) Virtual alignment of x-ray cone-beam tomography system using two calibration aperture measurements. *Optical Engineering* 38: 381–386.
12. Cho YB, Moseley DJ, Siewerdsen JH, Jaffray DA (2005) Accurate technique for complete geometric calibration of cone-beam computed tomography systems. *Medical Physics* 32: 968–983. <https://doi.org/10.1118/1.1869652> PMID: 15895580
13. Ford JC, Zheng DD, Williamson JF (2011) Estimation of CT cone-beam geometry using a novel method insensitive to phantom fabrication inaccuracy: Implications for isocenter localization accuracy. *Medical Physics* 38: 2829–2840. <https://doi.org/10.1118/1.3589130> PMID: 21815358
14. Noo F, Clackdoyle R, Mennessier C, White TA, Roney TJ (2000) Analytic method based on identification of ellipse parameters for scanner calibration in cone-beam tomography. *Physics in Medicine and Biology* 45: 3489–3508. PMID: 11098919
15. Robert N, Watt KN, Wang XY, Mainprize JG (2009) The geometric calibration of cone-beam systems with arbitrary geometry. *Physics in Medicine and Biology* 54: 7239–7261. <https://doi.org/10.1088/0031-9155/54/24/001> PMID: 19926916
16. Sun Y, Hou Y, Zhao FY, Hu JS (2006) A calibration method for misaligned scanner geometry in cone-beam computed tomography. *Ndt & E International* 39: 499–513.
17. von Smekal L, Kachelriess M, Stepina E, Kalender WA (2004) Geometric misalignment and calibration in cone-beam tomography. *Medical Physics* 31: 3242–3266. <https://doi.org/10.1118/1.1803792> PMID: 15651608
18. Yang K, Kwan ALC, Miller DF, Boone JM (2006) A geometric calibration method for cone beam CT systems. *Medical Physics* 33: 1695–1706. <https://doi.org/10.1118/1.2198187> PMID: 16872077
19. Gullberg GT, Tsui BMW, Crawford CR, Ballard JG, Hagius JT (1990) Estimation of Geometrical Parameters and Collimator Evaluation for Cone Beam Tomography. *Medical Physics* 17: 264–272. <https://doi.org/10.1118/1.596505> PMID: 2333053
20. Gullberg GT, Tsui BMW, Crawford CR, Edgerton ER (1987) Estimation of Geometrical Parameters for Fan Beam Tomography. *Physics in Medicine and Biology* 32: 1581–1594.
21. Khoury R, Bonissent A, Clémens JC, Meessen C, Vigeolas E, et al. (2009) A geometrical calibration method for the PIXSCAN micro-CT scanner. *Journal of Instrumentation* 4: 07016.
22. Panetta D, Belcarì N, Del Guerra A, Moehrs S (2008) An optimization-based method for geometrical calibration in cone-beam CT without dedicated phantoms. *Physics in Medicine and Biology* 53: 3841–3861. <https://doi.org/10.1088/0031-9155/53/14/009> PMID: 18583729
23. Rougssé A, Picard C, Ponchut C, Troussset Y (1993) Geometrical calibration of x-ray imaging chains for three-dimensional reconstruction. *Computerized Medical Imaging & Graphics the Official Journal of the Computerized Medical Imaging Society* 17: 295.
24. Ladikos A, Wein W. Geometric calibration using bundle adjustment for cone-beam computed tomography devices; 2012.

25. Meng Y, Gong H, Yang X (2013) Online Geometric Calibration of Cone-Beam Computed Tomography for Arbitrary Imaging Objects. *IEEE Transactions on Medical Imaging* 32: 278. <https://doi.org/10.1109/TMI.2012.2224360> PMID: 23076032
26. Panetta D, Belcari N, Del GA, Moehrs S (2008) An optimization-based method for geometrical calibration in cone-beam CT without dedicated phantoms. *Physics in Medicine & Biology* 53: 3841–3861.
27. Tekaya IB, Kaftandjian V, Buyens F, Sevestre S, Legoupil S (2013) Registration-Based Geometric Calibration of Industrial X-ray Tomography System. *IEEE Transactions on Nuclear Science* 60: 3937–3944.
28. Li X, Da Z, Liu B (2010) A generic geometric calibration method for tomographic imaging systems with flat-panel detectors—a detailed implementation guide. *Med Phys* 37: 3844–3854. <https://doi.org/10.1118/1.3431996> PMID: 20831092